

EXPERIMENTAL ANALYSIS OF BRITTLE FAILURE IN TIMBER-TO-STEEL CONNECTIONS WITH SMALL DIAMETER FASTENERS LOADED PARALLEL-TO-GRAIN

Miguel Yurrita. Wood Chair. Department of Building Construction, Services and Structures. University of Navarra. 31009 Pamplona, Spain. myurrital@alumni.unav.es

José Manuel Cabrero. Wood Chair. Department of Building Construction, Services and Structures. University of Navarra. 31009 Pamplona, Spain. jcabrero@unav.es

Hans Joachim Blaß. Timber Structures and Building Construction. Karlsruhe Institute of Technology. 76131 Karlsruhe, Germany. hans.blass@kit.edu

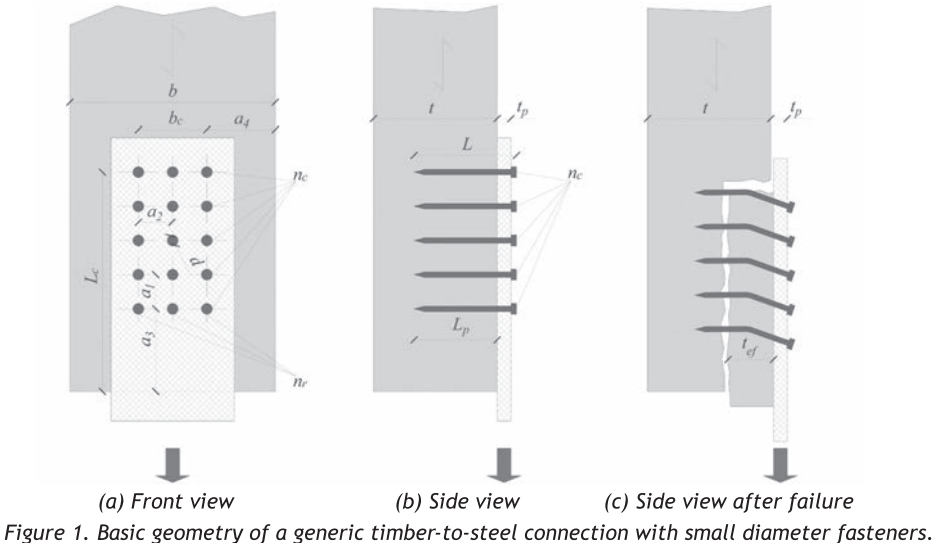
Note: This paper was originally published for INTER 2020

Keywords: Timber connection, Brittle failure, Experimental tests, Parallel-to-grain, Small diameter fastener, Plug shear

1 INTRODUCTION

Timber joints with steel fasteners are among the most used in timber construction. When the load-carrying capacity of the connection is reached, either a ductile (yielding of the fastener and embedment in the timber) or a brittle (crack of the wood) failure mode may occur. The reached failure mode depends on the materials of the connection and its geometry. Fig.1 depicts the geometry of a typical timber-to-steel connection with 15 (3 rows and 5 columns) small diameter fasteners (defined as those not protruding the whole timber thickness, such as nails, screws or rivets). The main geometrical parameters and the used nomenclature within this paper are included in Fig.1.

An accurate prediction of both ductile and brittle load-carrying capacities is of utmost importance to properly design timber connections. Traditionally, ductile failure mode has been considered by applying the European Yield Model (EYM), which in the *Eurocode 5* (2004), is combined with the reduction factor given by the effective number of fasteners n_{eff} , which includes some brittle failure modes such as splitting or row shear in the same calculation process. However, models dealing directly with brittle failure modes are included in the informative Annex A (for block shear and plug shear) in the *Eurocode 5* (2004).



In previous studies *Cabrero and Yurrita* (2018) analysed the existing models for brittle failure of connections. As a consequence, a model dealing with brittle failure mode of connections with large diameter fasteners loaded parallel-to-grain was proposed (*Yurrita and Cabrero* (2019) and *Yurrita and Cabrero* (2020)).

However, in the case of connections with small diameter fasteners, most of the available experimental results were based on rivet connections (*Foschi and Longworth* (1975), *Zarnani* (2013), *Zarnani and Quenneville* (2014), *Choquette* (2016)). It was required to improve the existing database of experimental test results with more tests in which nails and screws were used as fasteners. Therefore, as a preliminary step (similar to the work performed by *Yurrita, Cabrero, and Quenneville* (2019) for connections with large diameter fasteners), an experimental test campaign has been conducted in order to deeply analyse brittle failure in this kind of connections.

2 STATE OF THE ART

Fig.2 depicts the main brittle failure modes of timber connections with small diameter fasteners, such as nails, screws or rivets. Mode C (Fig.2c), namely plug shear, is the most representative. It is defined by the activation of three different failure planes, describing the perimeter of the wood within the fasteners: a head tensile plane H (with an area $A_{t,H} = t_{ep} b_c$), a bottom shear plane B (with an area $A_{v,B} = L_c b_c$) and two lateral shear planes L (with an area

$A_{v,L} = L_c t_{ep}$). Mode A (Fig. 2a) and Mode B (Fig.2b) are variants of plug shear in which the bottom shear B and the lateral shear planes L , respectively, are not activated.

Not all the existing models dealing with plug shear (Annex A from the *Eurocode 5* (2004), *Quenneville and Zarnani* (2017), *Kangas and Vesa* (1998), *Johnsson and Parida* (2013) and *Stahl et al.* (2004)) consider the three possible failure modes. All the models share the definition of the load-carrying capacity of each failure plane as its area multiplied by the corresponding strength (tensile parallel-to-grain f_t for the head tensile plane H , and shear strength f_v for the lateral and bottom shear planes). The difference between models consists on how the brittle capacity is obtained: in most cases, the load-carrying capacities of some or all failure planes are added. Table 1 provides an overview of the considered failure modes and the related failure planes by the existing models.

In the case of *Quenneville and Zarnani* (2017), a stiffness model considering those of each involved failure plane is used to obtain the load carrying capacity of the connection. In addition, they consider that both a brittle or a mixed failure can be achieved, depending on whether the crack of the wood happens before or after the yielding of the fastener. For that reason, a different effective thickness of the timber element t_{ep} that defines the depth of the head tensile H and the lateral L shear planes, is considered in both situations.

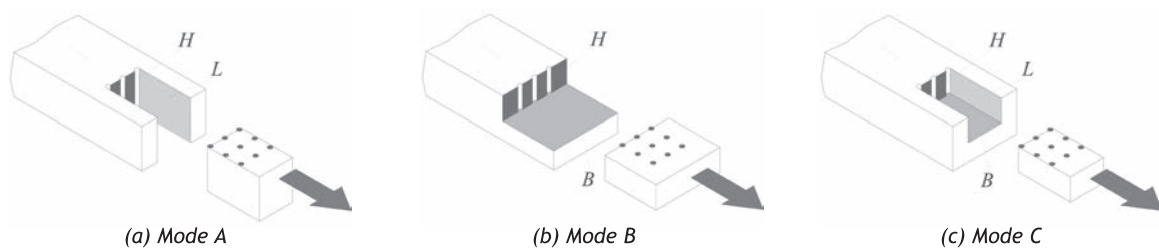


Figure 2. Failure modes with their loading planes (lateral shear L , bottom shear B and head tensile H).

Table 1. Summary of the existing brittle models for connections with small diameter fasteners.

Model	Mode A	Mode B	Mode C
<i>Stahl et al.</i> (2004)	$A_{v,L}f_v + A_{t,H}f_{t,0}$	$A_{v,B}f_v + A_{t,H}f_{t,0}$	$(A_{v,L} + A_{v,B})f_v + A_{t,H}f_{t,0}$
<i>Eurocode 5</i> (2004)	$\max \begin{cases} 1.5A_{t,H}f_{t,0} \\ 0.7A_{v,L}f_v \end{cases}$	—	$\max \begin{cases} 1.5A_{t,H}f_{t,0} \\ 0.7(A_{v,L} + A_{v,B})f_v \end{cases}$
<i>Kangas and Vesa</i> (1998)	—	—	$A_{v,B}f_v + A_{t,H}f_{t,0}$
<i>Johnsson and Parida</i> (2013)	—	—	$\max \begin{cases} A_{t,H}f_{t,0} \\ A_{v,B}f_v \end{cases}$
<i>Quenneville and Zarnani</i> (2017)	Stiffness approach	Stiffness approach	Stiffness approach

3 MATERIALS AND METHODS

A total of 34 different configurations (3 replicates per configuration, that is, 102 single tests) have been performed. Fig.3 depicts one specimen ready to be tested (Fig.3a) with its corresponding geometry (Fig.3b). All the specimens were designed with two symmetrical timber-to-steel connections. In all the connections, 15 fasteners were distributed in 3 rows and 5 columns, as depicted in the connection in Fig.1. The combination of different materials and variations of the connection geometry were used in order to study the influence of several parameters: timber product, fastener type, fastener slenderness L_p/d , steel plate thickness t_p , timber thickness t , distance to the lateral edge a_4 , distance to the end-loaded edge a_3 and the influence of pre-drilling the fasteners' holes.

With this purpose, two timber products were used: glulam GL28h and beech laminated veneer lumber

LVL80S. Table 2 includes the material properties used in the research. The characteristic values were obtained from EN14080 (2013) and EN14374 (2005) for GL28h and LVL80S, respectively. The given mean values, which were used for a pre-design of the specimens and to compare the obtained test results and the existing models (Section 5), were obtained following the procedure explained by Jockwer et al. (2018) and Cabrero, Honfi, et al. (2019), and based on the probabilistic model for timber proposed by the Joint Committee on Structural Safety (2006). The measured average timber density ρ_m (438-COV = 6.1% and 813-COV = 2.3%-kg/m³ for GL28h and LVL80S, respectively) is in good agreement with the values given in the standards.

The two different timber products were combined with two types of fasteners: nails and screws. To assess the influence of the fastener type, both types of fasteners were intended to be as similar as possible, both in length L (40, 60 and 75 mm for nails, and 40, 60 and 70

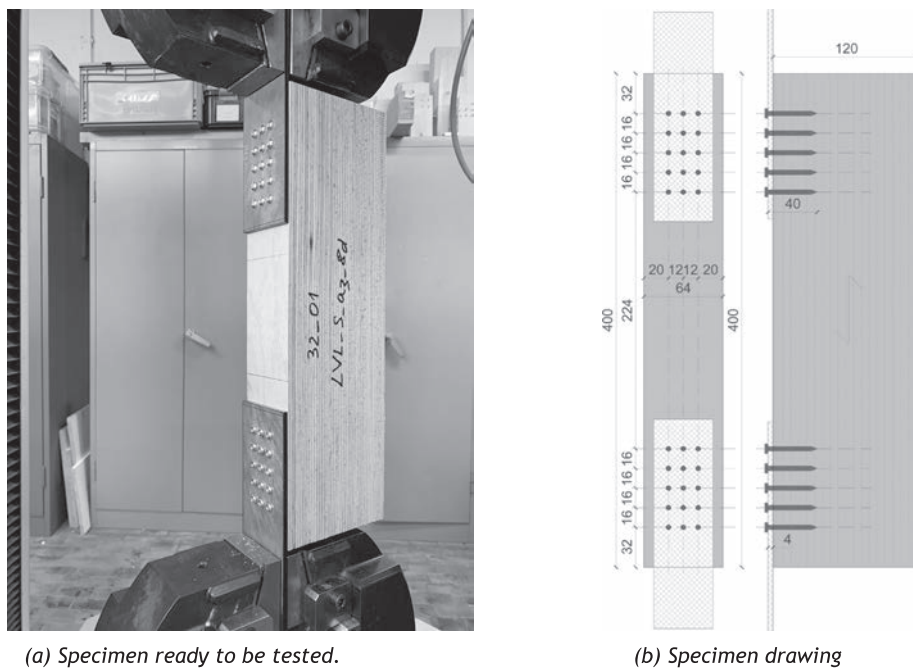


Figure 3. Test setup: example of an specimen of configuration LVL_S_a₃_8d.

Table 2. Material properties of the used timber products. Characteristic and mean values are given.

Timber product	$f_{t,0}$ [N/mm ²] ^a	f_v [N/mm ²] ^a	E_0 [N/mm ²] ^b	G [N/mm ²] ^b	ρ [kg/m ³] ^b
Characteristic level					
GL28h	22.3	3.5	10500	540	425
LVL80S	60	8	14900	630	730
Mean level					
GL28h	30.4	4.6	12600	650	460
LVL80S	75.5	10.4	16800	760	800

^a Mean level obtained by applying the parameters from Joint Committee on Structural Safety, 2006.

^b Mean level given in standards EN14080, 2013; EN14374, 2005.

mm for screws) and nominal diameters $d = 4$ mm (the screws had a core and outer diameters of 3 and 5 mm, respectively). The yield moment M_y provided from the manufacturer (6 500 N/mm for nails and 5 417 N/mm for screws) was considerably lower than the obtained experimental values (following the EN409 (2009)): 8 490-COV = 2.5%- and 7 090-COV = 2.2%- N/mm. Some authors already noticed that the actual yield strength may be higher than the one given by the manufacturers (Sandhaas et al. (2013); Blaß and Colling (2015)). All the steel plates were made of steel S235. According to the classification from the Eurocode 5 (2004), two types of steel plates were used: thin plates $-t_p/d \leq 0.5$ - ($t_p = 2$ mm) and thick plates $-t_p/d \geq 1$ - ($t_p = 4$ mm for GL28h and $t_p = 5$ mm for LVL80S).

The described materials were combined between them and with several geometrical variations, leading to 34 configurations expected to fail under plug shear. The geometrical and material properties of all the configurations are given in Table 3.

The connections were tested under tension parallel-to-the grain. The tension tests were performed following the standard ISO6891–1983 (1983). As shown in Fig.3a, two lines were drawn on each connection (one in the steel plate and another in the timber element) to measure the slip by means of an optical control system.

4 TEST RESULTS

The main failure mode of all the tested specimens was, as expected, plug shear. Fig.4 shows some of the test results. The obtained experimental values are given in Table 3. For each configuration, average values and the corresponding COV are given for the maximum load-carrying capacity F_T , the stiffness K_{ser} and the ductility D_f .

As each test included two symmetrical connections but commonly only one failed, the F_T values have been corrected by applying probabilistic model in which each test is considered as a two component Weibull system, as already done by Yurrita, Cabrero, and Quenneville (2019). The stiffness has been calculated by means of the slope of the loadslip curve between the 10% and the 40% of the maximum load.

Finally, the ductility D_f is defined by the ratio $D_f = \delta_f /$

δ_y (the yield displacement δ_y and the displacement of the point of the graphic where the maximum load F_T has been reached) as defined in EN12512 (2001), and used by several authors such as Ottenhaus et al. (2018), Jorissen and Fragiaco (2011) or Yurrita, Cabrero, and Quenneville (2019). Table 4 provides a brief overview of all these parameters. Four groups of configurations are given according to the two timber products and fastener types. In parallel, Fig.5 plots the relation between the load carrying capacity of the single tests with the stiffness K_{ser} (Fig.5a) and the ductility D_f (Fig.5b). In these graphics, the tests are divided into four groups corresponding to the combination of the two timber products with the fastener types.

It may be noticed how the tests with LVL80S reach in average higher load-carrying capacities and stiffness, but are more brittle (less ductility) than those with GL28h. Regarding the used fasteners, connections with screws withstand more load, are stiffer and, at the same time, are more ductile than the comparable ones with nails.

A classification of the tests regarding their ductility is also given in Table 4 and in (Fig.5b). As depicted in Fig.4b, in some cases, plug shear is combined with the yielding of the fasteners, which implies a mixed failure, as reported by Zarnani and Quenneville (2014). The classification of failure related to the achieved ductility proposed by Smith et al. (2006) is used. According to this scale, brittle failure implies a ductility $D_f \leq 2$, and ductile behaviour is considered when $D_f > 6$. In between, two intermediate stages, that can be considered as mixed failure, may be described: low ductility ($2 < D_f \leq 4$) and moderate ductility ($4 < D_f \leq 6$). This classification is given by means of vertical dashed lines in Fig. 5b. Most of the tests fall within the brittle (40.2%) and the low ductility (47.1%) ranges. The moderate ductility range gathers 10.8% of the tests specimens and only 2% of the test can be classified as ductile.

Regarding the failure process, it was noticed that not all the failure planes were activated simultaneously. Usually, the two lateral shear planes L started to fail first. Some of the tests even failed already at this initial stage, but most of them were able to withstand more load, until the head tensile H and bottom shear B planes failed, leading to the final failure of

Table 3. Material and geometrical properties of the tested configurations.

Configuration	Geometrical and material properties											Test Results								
	n_r	n_c	d [mm]	Fastener	L [mm]	Pre-drill	Timber	t_p [mm]	t [mm]	b [mm]	a_1/d	a_3/d	a_2/d	a_4/d	Aver.	COV	Aver.	COV	Aver.	COV
GL_N td_40	3	5	4	Nails	40	Yes	GL28h	4	120	64	4	12	3	5	28.25	5.2%	13.52	32.6%	1.56	9.3%
GL_N td_60	3	5	4	Nails	60	Yes	GL28h	4	120	64	4	12	3	5	36.8	5%	13.48	14.2%	1.91	40.5%
GL_N td_75	3	5	4	Nails	75	Yes	GL28h	4	120	64	4	12	3	5	36.87	5.6%	12.35	12.1%	1.55	13.1%
GL_N td_thin_40	3	5	4	Nails	40	Yes	GL28h	2	120	64	4	12	3	5	27.19	4%	15.4	3%	3.26	15%
GL_N td_thin_60	3	5	4	Nails	60	Yes	GL28h	2	120	64	4	12	3	5	35.92	3.6%	15.22	18.8%	3.25	35.7%
GL_N td_Np_40	3	5	4	Nails	40	No	GL28h	4	120	64	4	12	3	5	22.66	0.3%	11.23	17.7%	3.56	26.8%
GL_N td_Np_60	3	5	4	Nails	60	No	GL28h	4	120	64	4	12	3	5	27.06	2.6%	10.13	18.4%	2.1	13.9%
GL_N td_Np_75	3	5	4	Nails	75	No	GL28h	4	120	64	4	12	3	5	32.4	5.7%	11.51	17.5%	1.76	8.3%
GL_S td_40	3	5	4	Screws	40	Yes	GL28h	4	120	64	4	12	3	5	35.25	6.5%	19.99	25.7%	3.47	38.8%
GL_S td_60	3	5	4	Screws	60	Yes	GL28h	4	120	64	4	12	3	5	40.38	3.8%	15.97	21.5%	3.11	31.8%
GL_S td_70	3	5	4	Screws	70	Yes	GL28h	4	120	64	4	12	3	5	42.46	6.8%	17.23	17.5%	3.04	40.3%
GL_S td_thin_40	3	5	4	Screws	40	Yes	GL28h	2	120	64	4	12	3	5	35.25	5.5%	29.76	34.9%	6.16	43.8%
GL_S td_thin_60	3	5	4	Screws	60	Yes	GL28h	2	120	64	4	12	3	5	37.5	6.7%	17.9	30.3%	3.47	8%
GL_S td_Np_40	3	5	4	Screws	40	No	GL28h	4	120	64	4	12	3	5	28.63	3.3%	20.91	31.3%	3.58	37.7%
GL_S td_Np_60	3	5	4	Screws	60	No	GL28h	4	120	64	4	12	3	5	37.74	2.3%	24.95	31.4%	5.15	27%
GL_S td_Np_70	3	5	4	Screws	70	No	GL28h	4	120	64	4	12	3	5	42.28	13.7%	24.09	18.1%	4.47	36.5%
GL_N hw_60	3	5	4	Nails	40	No	GL28h	4	90	64	4	12	3	5	23.02	6.6%	12.44	12.4%	1.93	33.8%
GL_N hw_90	3	5	4	Nails	40	No	GL28h	4	90	64	4	12	3	5	23.12	14.6%	11.67	17%	2.41	49.1%
GL_S hw_60	3	5	4	Screws	40	No	GL28h	4	60	64	4	12	3	5	29.83	5.1%	15.09	20.9%	3.11	21.2%
GL_S hw_90	3	5	4	Screws	40	No	GL28h	4	90	64	4	12	3	5	31.6	1.1%	26.46	20.4%	3.92	38.4%
LV_N td_40	3	5	4	Nails	40	Yes	LV180S	5	120	64	4	12	3	5	57.38	0.8%	31.91	18.6%	1.99	14.2%
LV_N td_60	3	5	4	Nails	60	Yes	LV180S	5	120	64	4	12	3	5	63.21	2.8%	17.65	26.5%	2.19	36.3%
LV_N td_75	3	5	4	Nails	75	Yes	LV180S	5	120	64	4	12	3	5	62.5	51.7%	22.18	9.2%	2.39	34.1%
LV_S td_40	3	5	4	Screws	40	Yes	LV180S	5	120	64	4	12	3	5	64	11%	39.25	9.3%	2.73	27.7%
LV_S td_60	3	5	4	Screws	60	Yes	LV180S	5	120	64	4	12	3	5	68.16	6.3%	34.29	28.5%	2.34	2.4%
LV_S td_75	3	5	4	Screws	70	Yes	LV180S	5	120	64	4	12	3	5	72.49	2.7%	28.55	17.8%	2.38	31.1%
LV_N a4_7d	3	5	4	Nails	40	Yes	LV180S	5	120	80	4	12	3	7	58.23	3.5%	21.09	10.1%	1.65	16.6%
LV_N a4_9d	3	5	4	Nails	40	Yes	LV180S	5	120	96	4	12	3	9	56.85	3.2%	22.53	7.3%	1.27	10.2%
LV_S a4_7d	3	5	4	Screws	40	Yes	LV180S	5	120	80	4	12	3	7	67.2	8.4%	41.24	45.8%	2.27	28.8%
LV_S a4_9d	3	5	4	Screws	40	Yes	LV180S	5	120	96	4	12	3	9	65.91	1.6%	25.66	28.3%	1.99	31.2%
LV_N a3_8d	3	5	4	Nails	40	Yes	LV180S	5	120	64	4	8	3	5	54.07	7.3%	22.35	10.8%	1.47	25.9%
LV_N a3_16d	3	5	4	Nails	40	Yes	LV180S	5	120	64	4	16	3	5	60.79	2.1%	21.01	13.7%	1.75	36.4%
LV_S a3_8d	3	5	4	Screws	40	Yes	LV180S	5	120	64	4	8	3	5	59.93	5.9%	28.43	21.3%	1.75	10.7%
LV_S a3_16d	3	5	4	Screws	40	Yes	LV180S	5	120	64	4	16	3	5	64.89	0.5%	27.38	14.7%	2.21	7.5%

^a Corrected value according to the Weibull probabilistic model that considers the existence of two connections per test.

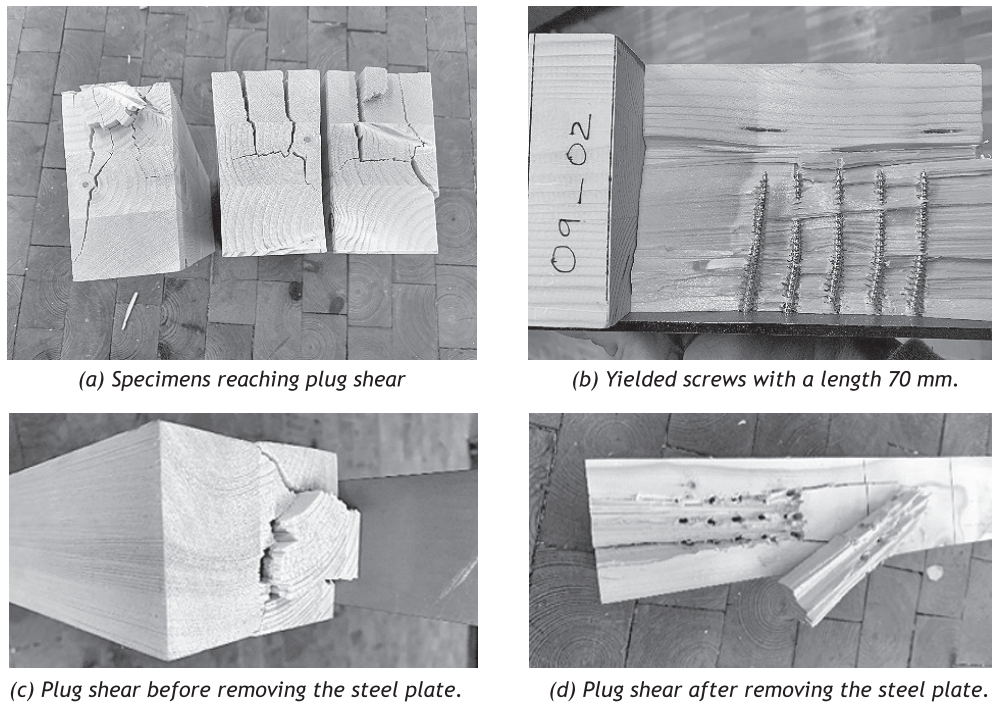


Figure 4. Images of the reached plug shear in the tested specimens

Table 4. Average values of load carrying capacity, stiffness and ductility of the performed test, and the % of cases for each ductility range (Smith et al. (2006)).

Tests studied	Aver. Load F_T [kN]	Aver. Stiffness K_{ser} [kN/mm]	Aver. Ductility D_f	Ductility ranges [%]			
				Brittle	Low duct.	Moderate duct.	Ductile
Tests with GL28h	32.03	15.57	3.08	25.8%	46.8%	17.7%	3.2%
Tests with LVL80S	61.02	26.57	2.03	57.5%	42.5%	0.0%	0.0%
Tests with Nails	40.29	16.24	2.13	47.6%	27.0%	3.2%	0.0%
Tests with Screw	47.71	23.93	3.15	23.1%	76.9%	23.1%	5.1%

the connection. This process is similar to the one described by Kangas and Vesa (1998) and Johnsson and Parida (2013).

The analysis of the studied parameters is given in Fig. 6. Each subfigure plots several groups of configurations (two or four, depending on the case) that include the variation of the studied parameter. The analysed

parameter is plotted in the abscissas axis, while the load-carrying capacity is given in the ordinates axis.

The fastener penetration length L_p , or the fastener slenderness L_p/d , is studied both in Fig.6a and Fig.6b. In general terms, the trend is clear: the load carrying capacity increases when the penetration length is increased. However, the observed non-linear

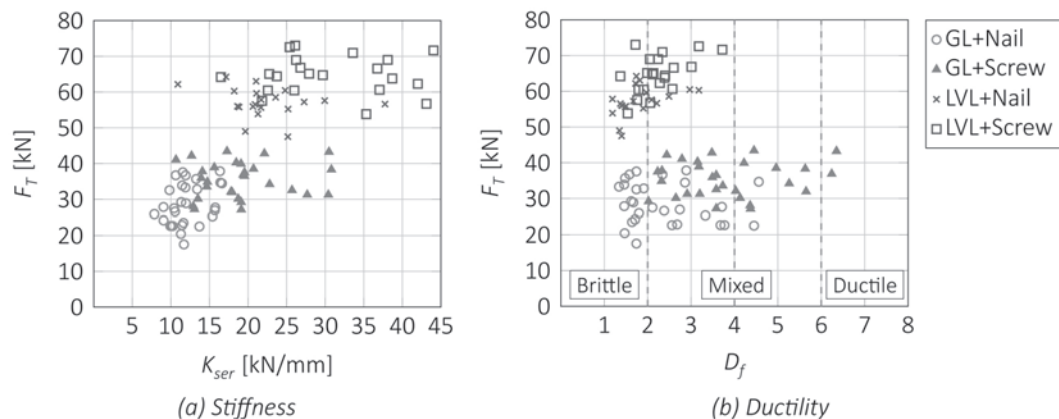


Figure 5. Analysis of the stiffness and ductility obtained in the tests. The test have been divided in 4 groups considering the 4 combinations of timber product and fastener type.

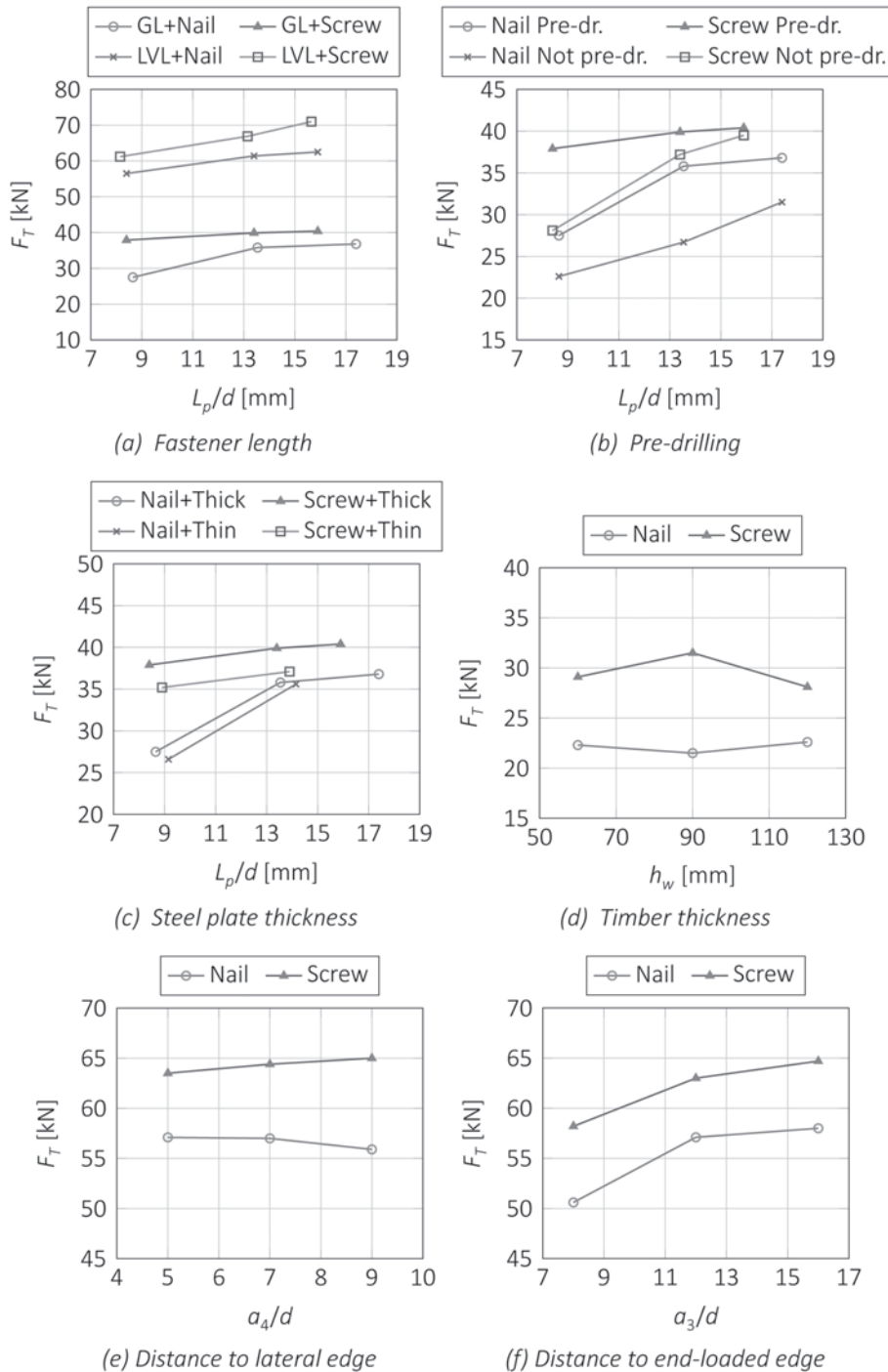


Figure 6. Analysis of the influence of the parameters considered in the tests.

tendency implies the necessity of defining an effective thickness t_{ef} that should consider both the elastic and plastic ranges of the fastener deformation for brittle and mixed failure, respectively.

Fig.6b also includes, by means of the plotted series, the influence of the pre-drilling of the fastener holes. When the pre-drilled and not pre-drilled series of each type of fasteners are compared, it may be seen how the pre-drilled cases (specially in stocky fasteners) reach a higher load-carrying capacity. As studied by

Blaß and Uibel (2009), this could be explained by the fact that the wood in between the fasteners becomes pre-stressed when there is no pre-drilling.

The influence of the steel plate thickness t_p is studied in Fig.6c, where configurations with thin and thick plates are plotted. Those cases with thick plates obtain slightly higher load capacities (around 3.5% for screws and 7.0% in nails). This variation is not so relevant to consider the steel plate thickness as a main parameter influencing in plug shear. In fact, *Görlacher*

(1995) demonstrated how the yielding behaviour of nails was always the expected for the cases of thick plates, no matter the used steel plate thickness.

The influence of the timber thickness t variation (keeping the same fastener penetration length L_p) is given in Fig.6d. The minimum variation of the load carrying capacity between the three tested cases (timber thickness of 60, 90 and 120 mm) suggests that the timber thickness is not a relevant parameter when the fastener penetration is kept the same.

Similar conclusions can be obtained from Fig.6e, where the influence of the distance to the lateral edge of the timber a_4 is studied. No clear trend (and low variation of results) may be noticed among the series of $5d$, $7d$ and $9d$. Therefore, a significant role of the distance a_4 in the load carrying capacity is discarded. It may only be relevant in order to avoid the failure mode in which the lateral shear planes are not activated (Fig.2b).

Finally, the influence of the distance to the loaded timber end a_3 is analysed in Fig.6f, considering cases of $8d$, $12d$ and $16d$. As expected, it is noticed that the increase of the a_3 distance implies an increase of the load-carrying capacity.

5 PERFORMANCE OF THE EXISTING MODELS

A brief comparison of the test results with the load carrying capacity predicted by the existing models has been performed (considering, as explained, the mean level of the material properties).

The prediction accuracy of the five models is plotted in Fig.7, by comparing the tested load-carrying capacity F_T (abscissas axis) with the predicted load F_p (ordinates axis). The ideal ratio $F_p/F_T = 1$ is given as a reference by means of a dashed line. A fitted linear regression passing through the origin of coordinates is provided, with the corresponding slope m coefficient of correlation R^2 .

The slopes closest to $m = 1$ are reached by the models from *Quenneville and Zarnani (2017)* (26.5% below) and the Annex A from the *Eurocode 5 (2004)* (20.8% above), obtaining both similar coefficients of correlation R^2 (around 0.68). *Kangas and Vesa (1998)* and *Johnsson and Parida (2013)* predict conservative average values (slopes of $m = 0.473$ and $m = 0.259$, respectively), while an opposite trend is provided by *Stahl et al. (2004)* ($m = 2.270$).

In Fig.8, a boxplot considering the ratio between the predicted and the tested load carrying capacity

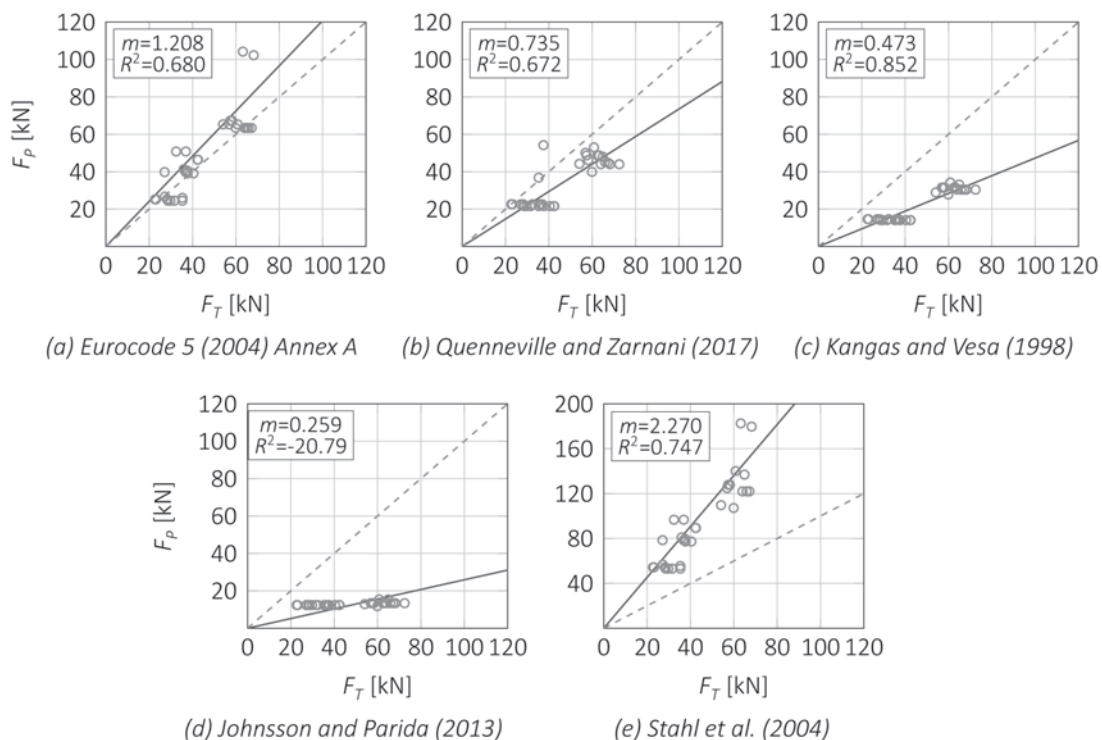


Figure 7. Comparison between the load capacity values obtained from the tests F_T and the corresponding theoretical values F_p predicted by the existing models.

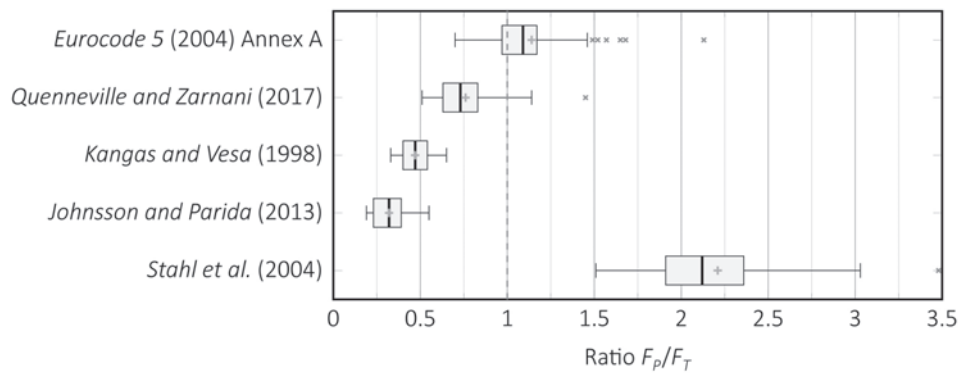


Figure 8. Boxplot considering the accuracy of the predicted ratio between the predicted failure load F_p and the tested failure load F_T .

F_p/F_T of each model is used to make a more direct comparison of the models' accuracy. Again, the ideal ratio $F_p/F_T = 1$ is given as a reference by means of a dashed line. In this case, both median (thick black lines) and average (crosses) values from the Annex A in the *Eurocode 5 (2004)* are the closest to the ideal ratio $F_p/F_T = 1$ with values around 1.12. However, this model has several outliers above the superior whisker. *Quenneville and Zarnani (2017)* provides average values around $F_p/F_T = 0.75$ and less scattered results (only one outlier). The scatter from both *Kangas and Vesa (1998)* and *Johnsson and Parida (2013)* is very low, but their average values are under $F_p/F_T = 0.5$. Finally, *Stahl et al. (2004)* obtains average and mean values above $F_p/F_T = 2$ and the largest box and whiskers (highest scatter)

6 CONCLUSIONS AND FUTURE WORK

An experimental test campaign of timber-to-steel connections with small diameter fasteners loaded in tension parallel-to-grain has been conducted in order to study brittle failure (plug-shear). Different materials (timber -GL28h and LVL80S- and fasteners -nails and screws-) and geometries are combined to identify the main parameters that have an influence on the load-carrying capacity of the connection.

The obtained test results confirmed plug shear as the main failure mode. It is noticed that the failure of all the loading planes does not happen at the same time: first, the lateral shear planes L are activated; and then, only if the connection is able to withstand more load, the head tensile H and the bottom B shear planes fail.

Regarding the ductility D_r , both brittle and mixed failure are reached. The least brittle cases usually

correspond to configurations that combine screws with GL28h. Configurations with screws combined with LVL80S usually reach both the highest average load-carrying capacity and stiffness values.

The analysis of the test results provides information on the influence of different parameters. Some of them are confirmed to have an influence (such as timber product, fastener type, spacings, fastener slenderness, or the pre-drilling of the holes), while others seem not to have a clear influence (steel plate thickness and timber thickness).

Finally, the comparison of the test results with the predicted values from the existing models dealing with plug-shear helps to identify some aspects to be improved. With all this new knowledge, further work would try to provide a new model which could improve the prediction accuracy by including the analysed influencing parameters.

7 ACKNOWLEDGMENTS

The research has been performed thanks to the network formed within the COST Action FP1402. The first author is supported by a PhD fellowship from the Programa de Becas FPU del Ministerio de Educación y Ciencia (Spain) under the grant number FPU15/03413. He would also like to thank the Asociación de Amigos (University of Navarra) for their help with a fellowship in early stages of this research. The stay of the first author in the Karlsruhe Institute of Technology has been supported by a fellowship from Gobierno de Navarra. All the authors would like to acknowledge the contribution of the Holzbau und Baukonstruktionen from the Karlsruhe Institute of Technology for funding and performing the tests.

8 REFERENCES

- Blaß, H. J. and Colling, F. (2015). "Load-carrying capacity of dowelled connections". In: *International Network Timber Engineering Research*. Šibenik, Croatia, Paper 48-7-3.
- Blaß, H. J. and Uibel, T. (2009). *Spaltversagen von Holz in Verbindungen - Ein Rechenmodell für die Rissbildung beim Eindrehen von Holzschrauben*. German. Tech. rep. doi:10.5445/KSP/1000009896. Karlsruher Institut für Technologie (KIT). 180 pp.
- Cabrero, J. M. and Yurrita, M. (2018). "Performance assessment of existing models to predict brittle failure modes of steel-to-timber connections loaded parallel-to-grain with dowel-type fasteners." In: *Engineering Structures* 171. doi:10.1016/j.engstruct.2018.03.037, 895-910 (INTER version 51-7-12).
- Cabrero, J. M., Honfi, D., Jockwer, R., and Yurrita, M. (2019). "A probabilistic study of brittle failure in dowel-type timber connections with steel plates loaded parallel to the grain". In: *Wood Material Science & Engineering* 14.5. doi:10.1080/17480272.2019.1645206, pp. 298-311.
- Choquette, J. (2016). "Évaluation d'une nouvelle méthode de calcul des assemblages de bois à l'aide de connecteurs de petits diamètres". MA thesis. Université Laval, Québec, Canada.
- EN12512 (2001). *Timber structures. Test methods. Cyclic testing of joints made with mechanical fasteners*. Comité Européen de Normalisation.
- EN14080 (2013). *Timber structures - Glued laminated timber and glued solid timber - Requirements*. Comité Européen de Normalisation.
- EN14374 (2005). *Timber structures - Structural laminated veneer lumber - Requirements*. Comité Européen de Normalisation.
- EN409 (2009). *Timber structures - Test methods - Determination of the yield moment of dowel type fasteners*. Comité Européen de Normalisation.
- Eurocode 5 (2004). *CEN:EN 1995-1-1:2004 - Eurocode 5: Design of timber structures - Part 1-1: General - Common rules and rules for buildings*. CTN.
- Foschi, R. O. and Longworth, J. (1975). "Determining embedment response parameters from connector tests". In: *Journal of the Structural Division* 101, pp. 2537-2555.
- Görlacher, R. (1995). "Load-carrying capacity of steel-to-timber joints with annular ringed shank nails". In: *CIB-W18 Timber Structures*. Copenhagen, Denmark, Paper 28-7-3.
- ISO6891-1983 (1983). *Timber structures - Joints made with mechanical fasteners - General principles for the determination of strength and deformation characteristics*. ISO/TC 165.
- Jockwer, R., Fink, G., and Köhler, J. (2018). "Assessment of the failure behaviour and reliability of timber connections with multiple dowel-type fasteners". In: *Engineering Structures* 172. doi:10.1016/j.engstruct.2018.05.081, pp. 76-84.
- Johnsson, H. and Parida, G. (2013). "Prediction model for the load-carrying capacity of nailed timber joints subjected to plug shear". In: *Materials and Structures* 46.12. doi:10.1617/s11527-013-0030-8, pp. 1973-1985. ISSN: 1359-5997.
- Joint Committee on Structural Safety, ed. (2006). *Probabilistic Model Code*. JCSS. Chap. 3.5. Properties of Timber.
- Jorissen, A. J. and Fragiaco, M. (Nov. 2011). "General notes on ductility in timber structures". In: *Engineering Structures* 33.11. doi:10.1016/j.engstruct.2011.07.024, pp. 2987-2997. ISSN: 01410296.
- Kangas, J. and Vesa, J. (1998). "Design on timber capacity in nailed steel-to-timber joints". In: *CIB-W18 Timber Structures*. Savonlinna, Finland, Paper 31-7-4.
- Ottenhaus, L.-M., Li, M., Smith, T., and Quenneville, P. (2018). "Mode cross over and ductility of dowelled LVL and CLT connections under monotonic and cyclic loading". In: *Journal of Structural Engineering* 144.7. doi:10.1061/(ASCE)ST.1943-541X.0002074.

- Quenneville, P. and Zarnani, P. (2017). *Proposal for the Connection Chapter of the New Zealand Design of Timber Structures*. Unpublished.
- Sandhaas, C., Ravenshorst, G. J. P., Blass, H. J., and Van De Kuilen, J. W. G. (2013). "Embedment tests parallel-to-grain and ductility aspects using various wood species". In: *European Journal of Wood and Wood Products* 71.5. doi:10.1007/s00107-013-0718-z, pp. 599-608. ISSN: 00183768.
- Smith, I., Asiz, A., Snow, M., and Chui, Y. H. (2006). "Possible Canadian/ISO approach to deriving design values from test data". In: *CIB W18 Timber Structures*. Florence, Italy, Paper 39-17-1.
- Stahl, D. C., Wolfe, R. W., and Begel, M. (2004). "Simplified analysis of timber rivet connections". In: *Journal of Structural Engineering* 130.August, pp. 1272-1279. ISSN: 0733-9445. DOI: 10.1061 (ASCE)0733-9445(2004)130:8(1272).
- Yurrita, M. and Cabrero, J. M. (2020). "New design model for brittle failure in the parallel-to-grain direction of timber connections with large diameter fasteners". In: *Engineering Structures* 217. doi:10.1016/j.engstruct.2019.109959, (INTER version 52-7-5).
- Yurrita, M., Cabrero, J. M., and Quenneville, P. (May 2019). "Brittle failure in the parallel-to-grain direction of multiple shear softwood timber connections with slotted-in steel plates and dowel-type fasteners". In: *Construction and Building Materials* 216. doi:10.1016/j.conbuildmat.2019.04.100, pp. 296-313 (INTER version 51-7-10).
- Zarnani, P. (2013). "Load-Carrying Capacity and Failure Mode Analysis of Timber Rivet Connections". PhD thesis. University of Auckland, p. 225.
- Zarnani, P. and Quenneville, P. (2014). "Strength of timber connections under potential failure modes: An improved design procedure". In: *Construction and Building Materials* 60. doi:10.1016/j.conbuildmat.2014.02.049, pp. 81-90. ISSN: 09500618.
-